ARMY RESEARCH LABORATORY

The Effect of Fuel Injector Nozzle Configuration on JP-8 Sprays at Diesel Engine Conditions

by Matthew Kurman, Luis Bravo, Chol-Bum Kweon, and Michael Tess

ARL-RP-0510 **October 2014**

Reprinted from ILASS-Americas [accessed 2014 Oct 10]. http://www.ilass.org/2/conferencepapers/36_2014.pdf. Paper presented at: ILASS Americas 26th Annual Conference on Liquid Atomization and Spray Systems; 2014 May; Portland, OR.

NOTICES

Disclaimers

The findings in this report are not to be construed as an official Department of the Army position unless so designated by other authorized documents.

Citation of manufacturer's or trade names does not constitute an official endorsement or approval of the use thereof.

Destroy this report when it is no longer needed. Do not return it to the originator.

Army Research Laboratory
Aberdeen Proving Ground, MD 21005-5066

ARL-RP-0510 **October 2014**

The Effect of Fuel Injector Nozzle Configuration on JP-8 Sprays at Diesel Engine Conditions

Matthew Kurman, Luis Bravo, and Chol-Bum Kweon
Vehicle Technology Directorate, ARL

Michael Tess
University of Wisconsin-Madison

Reprinted from ILASS-Americas [accessed 2014 Oct 10]. http://www.ilass.org/2/conferencepapers/36_2014.pdf. Paper presented at: ILASS Americas 26th Annual Conference on Liquid Atomization and Spray Systems; 2014 May; Portland, OR.

REPORT DOCUMENTATION PAGE

Form Approved
OMB No. 0704-0188

1. REPORT DATE *(DD-MM-YYYY)*	2. REPORT TYPE	3. DATES COVERED (From - To)
October 2014	Reprint	January 2014–March 2014

4. TITLE AND SUBTITLE
The Effect of Fuel Injector Nozzle Configuration on JP-8 Sprays at Diesel Engine Conditions

5a. CONTRACT NUMBER

5b. GRANT NUMBER

5c. PROGRAM ELEMENT NUMBER

6. AUTHOR(S)
Matthew Kurman, Luis Bravo, Chol-Bum Kweon, and Michael Tess

5d. PROJECT NUMBER

5e. TASK NUMBER

5f. WORK UNIT NUMBER

7. PERFORMING ORGANIZATION NAME(S) AND ADDRESS(ES)
US Army Research Laboratory
ATTN: RDRL-VTP
Aberdeen Proving Ground, MD 21005-5066

8. PERFORMING ORGANIZATION REPORT NUMBER
ARL-RP-0510

9. SPONSORING/MONITORING AGENCY NAME(S) AND ADDRESS(ES)

10. SPONSOR/MONITOR'S ACRONYM(S)

11. SPONSOR/MONITOR'S REPORT NUMBER(S)

12. DISTRIBUTION/AVAILABILITY STATEMENT
Approved for public release; distribution is unlimited.

13. SUPPLEMENTARY NOTES
Reprinted from ILASS-Americas [accessed 2014 Oct 10]. http://www.ilass.org/2/conferencepapers/36_2014.pdf. Paper presented at: ILASS Americas 26th Annual Conference on Liquid Atomization and Spray Systems; 2014 May; Portland, OR.

14. ABSTRACT
The effect of injector nozzle configuration on liquid and vapor penetration lengths of JP-8 sprays was investigated. Non-reacting spray experiments were conducted in a high temperature (900 K), high pressure (60 bar) flow-through chamber which simulates realistic conditions found in compression-ignition engines. Three different Bosch CRIN3 fuel injectors consisting of a 1-hole axial, a 2-hole adjacent (spaced 60°), and a 6-hole (spaced 60°) nozzle configuration were used for the study. Prior to conducting the spray studies, each fuel injector was mapped with an injection analyzer to ensure consistent fuel delivery between injectors. For the experiments, fuel rail pressure was maintained at 1000 bar at two different fuel injection durations consisting of 0.45 ms and 0.7 ms, representing low and high loads. High-speed Mie and schlieren images were acquired and processed using LaVision software for the three different nozzle configurations. Furthermore, high-speed axial Mie scattering images were acquired for the 2 and 6-hole injectors. Results show that the 1-hole and 6-hole injectors have a quasi-steady liquid penetration length of 20 mm and for the 2-hole injector the liquid length was 15 mm. Results from the injector mapping revealed that fuel mass does not scale linearly with the increase in the number of orifices. The liquid penetration rate was similar for the 1 and 2-hole injectors, however, slower for the 6-hole injector. Plume to plume liquid length variations were present for both the 2 and 6-hole injectors. However, the 6-hole presented more variations than the other injectors tested. In addition, a 3D CFD study was conducted to compare modeling to experimental results. Fuel spray studies investigating liquid and vapor penetrations lengths can be useful to increase atomization and vaporization, thus ultimately improving combustion and fuel efficiency.

15. SUBJECT TERMS
JP-8, Mie, schlieren, diesel, non-reacting

16. SECURITY CLASSIFICATION OF:			17. LIMITATION OF ABSTRACT	18. NUMBER OF PAGES	19a. NAME OF RESPONSIBLE PERSON
a. REPORT	b. ABSTRACT	c. THIS PAGE			Matthew S Kurman
Unclassified	Unclassified	Unclassified	UU	20	19b. TELEPHONE NUMBER (*Include area code*) 410-278-8971

Standard Form 298 (Rev. 8/98)
Prescribed by ANSI Std. Z39.18

The Effect of Fuel Injector Nozzle Configuration on JP-8 Sprays at Diesel Engine Conditions

Matthew Kurman*, Luis Bravo, and Chol-Bum Kweon
U.S. Army Research Laboratory, Aberdeen Proving Ground, MD 21005
&
Michael Tess
University of Wisconsin-Madison, Madison, WI 53706

Abstract

The effect of injector nozzle configuration on liquid and vapor penetration lengths of JP-8 sprays was investigated. Non-reacting spray experiments were conducted in a high temperature (900 K), high pressure (60 bar) flow-through chamber which simulates realistic conditions found in compression-ignition engines. Three different Bosch CRIN3 fuel injectors consisting of a 1-hole axial, a 2-hole adjacent (spaced 60°), and a 6-hole (spaced 60°) nozzle configuration were used for the study. Prior to conducting the spray studies, each fuel injector was mapped with an injection analyzer to ensure consistent fuel delivery between injectors. For the experiments, fuel rail pressure was maintained at 1000 bar at two different fuel injection durations consisting of 0.45 ms and 0.7 ms, representing low and high loads. High-speed Mie and schlieren images were acquired and processed using LaVision software for the three different nozzle configurations. Furthermore, high-speed axial Mie scattering images were acquired for the 2 and 6-hole injectors. Results show that the 1-hole and 6-hole injectors have a quasi-steady liquid penetration length of 20 mm and for the 2-hole injector the liquid length was 15 mm. Results from the injector mapping revealed that fuel mass does not scale linearly with the increase in the number of orifices. The liquid penetration rate was similar for the 1 and 2-hole injectors, however, slower for the 6-hole injector. Plume to plume liquid length variations were present for both the 2 and 6-hole injectors. However, the 6-hole presented more variations than the other injectors tested. In addition, a 3D CFD study was conducted to compare modeling to experimental results. Fuel spray studies investigating liquid and vapor penetrations lengths can be useful to increase atomization and vaporization, thus ultimately improving combustion and fuel efficiency.

*Corresponding author: matthew.s.kurman.civ@mail.mil

Introduction

Fundamental physical understanding of spray atomization process is critical in improving engine performance and efficiency as well as complying with strict emissions standards for optimum power and reduction of exhaust gases and particulates. Spray technology has a wide range of applications in military technologies such as combustion devices found in unmanned aerial systems (rotary and piston engines), aerospace propulsion systems (gas turbine engines), and ground vehicle engines (piston engines) [1, 2]. Hence, a detailed characterization of the spray and combustion processes is important in driving the understanding and development of new technologies for single fuel concept JP-8 optimized engines for Army battlefield operations.

Several detailed studies of the spray process exist in the combustion literature focusing on the atomization and breakup characteristics of engine sprays through the use of combustion vessels [3-5]. The Engine Combustion Network (ECN), established through the efforts at Sandia National Laboratories (SNL), has historically driven the experimental efforts in quantifying spray parameters with the aim of providing insights and growing a high-fidelity consolidated database at diesel and gasoline engine relevant conditions. An excellent review has been published focusing on the comparison between the operations and control of boundary conditions in Constant-Volume Preburn (CVP) and Constant-Pressure Flow (CPF) chambers while studying a well reported case denoted as Spray A [5]. The Spray A condition was developed in an effort to standardize testing among the ECN group participants and to leverage expertise, while enabling direct comparison between experiments. Ambient conditions were selected to represent a typical diesel engine combustion event at 900 K, 60 bar (injection pressure of 1500 bar) at 0% O_2 and 15% O_2 conditions for non-reacting and reacting sprays.

Using a CVP chamber and diesel fuel, the effect of injector parameters and conditions on liquid and vapor penetration lengths was reported [6]. It was established that liquid length decreases with a decrease in orifice diameter, an increase in ambient temperature or ambient density, and an increase in fuel volatility or fuel temperature. In addition, the liquid length is weakly dependent on fuel injection pressure suggesting that the change in fuel mass flow rate with the change in injection pressure causes fuel vaporization to change at a similar rate. Empirical models (zero order) validated across several conditions mainly for engineering calculations were proposed. Also at the Spray A condition, work was presented for reacting and non-reacting CVP chamber spray measurements with JP-8 and diesel fuel to study the effects of the fuel's physical/chemical variations on spray parameters [7].

Shorter liquid penetration lengths, when compared to diesel fuel, were observed due to higher fuel volatility of JP-8 with no apparent effect on vapor length and spreading angle. Ignition delay measurements were 25%-50% higher than diesel indicating strong chemical differences between fuels and possibly faster mixing of JP-8. In a more recent study, experiments were conducted at the Spray A condition with six fuels including conventional (No. 2 Diesel, JP-8, Jet-A), alternative fuels, and a surrogate with the objective of assessing the performance of alternative fuels in diesel engines [8]. Several differences in liquid penetration lengths arising from variations in fuel volatility and density were reported with peak liquid penetration lengths reported with No. 2 Diesel (max) and Fischer-Tropsch/surrogate (min). Variations in vapor penetration and spreading angles were not significant in the observations suggesting the mixing and entrainment process among all fuels was not significantly affected.

In addition to single-hole nozzle studies, multi-hole nozzle spray measurements are gaining recent attention in part due to their direct link with production injectors. An eight-hole injector was used to provide diesel sprays and vaporization was reported [9]. The research showed significant plume to plume variations in liquid penetration during the transient and steady phases under repeated test conditions including a charge temperature sweep. The asymmetries from peak-to-peak were reported as 18% for repeat test conditions, and 15% for temperature sweep tests. The variations were thought to arise from eccentric needle motion (wobble) in the nozzle affecting the distribution of the fuel flow. Although orifice-hole variations in this study were not considered a factor in resolving the penetration length differences, more recent studies have emphasized the importance of characterizing the injectors in detail. The methodology for characterization, including high-resolution CT-scan imaging is presented in detail [10, 11]. The studies report asymmetric orifice, eccentric bilateral needle motion and its effect on liquid penetration profiles.

In this study, 3 different Bosch CRIN3 fuel injectors consisting of 1-hole axial, 2-hole adjacent, and 6-hole fuel injectors are used to provide JP-8 sprays in a 900 K temperature, 60 bar pressure environment. Liquid and vapor penetration lengths are analyzed and spray plume variations between injector nozzle configurations are examined. In addition, a computational fluid dynamics (CFD) analysis is conducted to provide insights into JP-8 spray interaction.

Experimental Setup

JP-8 spray experiments were conducted in a stainless-steel high temperature pressure vessel (HTPV) flow-through chamber as shown in Figure 1. The HTPV is designed to reach a maximum pressure of 150 bar and a maximum temperature of 1000 K. However, for the experiments discussed in this study the HTPV

was operated at 900 K and 60 bar. These ambient conditions are typical for a compression-ignition engine. The nitrogen is heated by a 2-stage cartridge heater and a ceramic heater in the inlet section of the vessel. The vessel is equipped with closed-loop control for pressure and temperature. Flow through the chamber is held constant at 58.0 m^3/hr. An on-site nitrogen generator produced the necessary nitrogen for testing, which was maintained at 99% purity during experiments. To allow for optical access, the vessel is outfitted with 3 fused silica windows with dimensions of 147 mm diameter by 85 mm thickness. To protect the 85 mm thick pressure windows from fuel contamination or flames (during combustion experiments), 6 mm thick fused silica windows are placed between the 85 mm windows and the spray/combustion zone.

High-speed near simultaneous Mie and schlieren images were acquired with a Photron SA5 camera, operating at 60,000 fps, equipped with a 100 mm Zeiss Makro-Planar f/2 prime lens. For the experiments presented, image size was set to 320 by 320 pixels and the corresponding scaling was 0.25 mm/pixel. The Mie/schlieren system consists of a folded z-type arrangement in which the liquid portion of the spray can be detected by Mie scattering of the light and the vapor boundary of the evaporated spray can be imaged by the schlieren system. The experimental diagnostics are shown in Figure 1. Camera exposure time for the recordings was set to 16 us. Mie and schlieren images were near simultaneously acquired utilizing a frame straddling technique similar to the method described in other work [12]. A representative timing diagram is shown in Figure 2. This imaging technique allows for alternating light sources, with a light duration of 10 us for the Mie scattering and 5 us for the schlieren images, to be used during the recording. Light for the schlieren images is produced from a single LED, and then is diffused through a 1500 grit ground glass diffuser to eliminate the structure of the LED source. The diffused light is focused to a point by using a 40 mm aspheric condenser lens and an adjustable aperture is used to adjust the size of the point source. The light is then collimated by a 152.4 mm diameter, f/8 parabolic mirror and directed to a 152.4 mm flat folding mirror aligned to project the collimated light into the HTPV. The light reaches another 152.4 mm diameter flat mirror and is directed to an additional 152.4 mm diameter, f/8 parabolic mirror that projects the light to a razor blade knife edge and the high speed camera. Light for the Mie scattering images is provided by a 24 LED array light source that is placed at a slight angle from the axial position of the fuel injector. Timing of the camera system and light sources is controlled by a DG645 digital delay/pulse generator which is triggered from the fuel injector command. In addition, axial Mie scattering experiments were conducted with the 2-hole and 6-hole injectors to image the liquid portion of the spray at a higher frame rate and a larger pixel to length ratio. For the axial Mie experiments presented, the camera was operated at 80,000 fps with a resolution of 256 by 256 pixels with the same lens previously mentioned. For this setup, the corresponding scaling was 0.11 mm/pixel. The LED array was used as the light source for the experiments and was orthogonal to the camera. In order to compare axial images of the 6-hole to the 2-hole, the region of interest on the 6-hole injector was the spray plumes that correspond to the 2 plumes on the 2-hole injector.

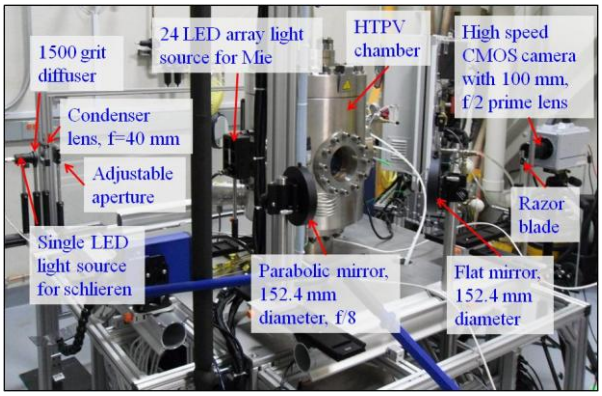

Figure 1. High temperature pressure vessel facility shown with Mie and schlieren diagnostics.

Image Analysis

Image processing was conducted with LaVison DaVis imaging software. During the experiments, the schlieren system was adjusted with a large light cutoff to increase the sensitivity of the system. With an increase in sensitivity, background or unwanted schlieren effects were present. These effects can be removed during the post-processing analysis. Background subtraction was conducted with the raw image by subtracting the image prior to the start of injection. In addition, background subtraction of the frame prior to the frame of interest was conducted similarly to the method described elsewhere [13]. This eliminates the background schlieren effects for the schlieren images. Background subtraction was also conducted for the Mie images to remove any unwanted light reflections from the injector tip and injector holder. A 3% threshold was applied to the resulting image to determine the penetration limits.

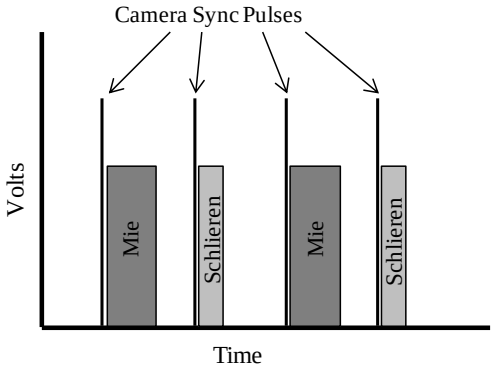

Figure 2. Timing diagram showing the camera sync signal and Mie and schlieren light source durations.

Fuel Injection System and Injector Characterization

The fuel injection system consists of a high-pressure fuel bench connected to a common rail. The high-pressure fuel bench contains an OEM fuel pump which is operated by an electric motor. Maximum fuel rail pressure for this fuel bench system is set at 1800 bar and is maintained constant by closed-loop control. For the experiments presented, fuel rail pressure was held constant at 1000 bar. The motor speed is maintained by a variable frequency drive. Fuel injection events were controlled by a Drivven direct injector (DI) driver system. Total energizing times for the presented experiments were 450 us and 700 us. Current profiles of the injectors were measured with a current probe connected to an oscilloscope with a recording time step of 1 us. Table 1 shows the injector settings used for this study.

Stage	**1**	**2**	**3**
Set Current [A]	23	15	11
Upper Current [A]	23.5	15.5	11.5
Lower Current [A]	22.5	14.5	10.5
Duration [ms]	0.13	0.3	balance

Table 1. Injector current and time settings.

The Bosch CRIN3 fuel injectors tested in this study consisted of 3 different injectors each having a different nozzle configuration. The nozzles were OEM and were modified for different configurations. Each orifice diameter was 147 um. The nozzle configurations include a 1-hole, 2-hole adjacent with 60° separation, and a 6-hole spaced 60° separation. For the 1-hole nozzle all stock 6-holes were welded and an axial orifice was created by electrical discharge machining (EDM). For the 2-hole adjacent nozzle, 4 holes were welded and the other 2 remained unchanged. No modifications to the 6-hole injector were performed. Before conducting the experiments with the 2-hole and 6-hole injectors, the injector was oriented so that an orifice was in the vertical direction inside the HTPV.

Prior to testing in the HTPV, each fuel injector was tested and mapped in an IAV fuel injection analyzer to determine the injected fuel mass. The injection analyzer operates on the principle that the mass of fuel is related to the speed of sound in the fluid by the following relationship,

$$m = \frac{A_t}{a} \int p(t) dt, \quad (1)$$

where A_t is the cross-sectional area of the tube, a is the fluid sound speed, and $p(t)$ is the dynamic pressure as a function of time in the tube. 100 shot averages of the injected fuel mass and rate of injection profiles were acquired with the injection analyzer. In addition, to supplement the injected fuel mass results from the injection analyzer, a precision scale was used to measure the injected fuel mass from each injector. The scale method does not provide a shot to shot analysis and only provides an average of the total injections. For this study, 200 shots were used to determine the average.

Numerical Simulations

The numerical simulation solver, CONVERGE developed by Convergent Science, Inc., has been adopted and utilized here for the modeling of evaporating sprays. CONVERGE is a compressible Navier Stokes solver based on a first-order predictor-corrector time integration scheme, featuring a choice of second or higher order finite volume schemes for spatial discretization. An efficient geometric multi-grid treatment is used to solve the pressure equation in a non-staggered, collocated, computational grid framework. Domain parallelization is based on implementations of OpenMPI or Message Passing Interface (MPI) protocols. It provides the option of increasing resolution locally and dynamically by way of Adaptive Mesh Refinement (AMR) activated and controlled through user specified criteria. Spray modeling in this work, is achieved by making use of Eularian Lagrangian formulations based on Kelvin Helmholtz - Raleigh Taylor (KH-RT) model. The solver also provides several modeling options for the treatment of turbulence, including large eddy simulation (LES), and Reynolds Average Navier Stokes (RANS) models.

In this study, numerical simulations have been carried out in an effort to present additional information of the underlying dynamics found in evaporating sprays. Both cases, 1-hole and 2-hole nozzles, have been considered to report on the spray formation process in terms of global diagnostics, liquid and vapor length, for the injection duration of 0.7 ms. A liquid fuel surrogate, denoted Modified Aachen, has been adopted in this study to model JP-8 properties. In a

related study, surrogates have been interrogated showing good overall agreement and similar atomization behavior [14]. A resolution level of dx = 0.0625 mm cell size, an embed scale of 5, with total injected 800,000 particles has been utilized with a value of nozzle-to-grid ratio of 2.352. For all studies, a high-resolution LES approach was utilized making use of up to 9 LES cycles to conduct averaging for shot-to-shot quantities. The approach was based on previous work where it was reported that a total of 9 cycles were needed as the minimum number of LES realizations to maintain a reasonable representation of the average spray behavior for the Spray A configuration. The average of 9 LES realizations yields absolute errors of less than +/- 2.0 m/s for velocity and 0.005 for mixture fraction, 95% of the time [15].

Computed Tomography of Injector Nozzles

Characterization of the internal geometry of the fuel injectors was conducted by utilizing computed tomography (CT) imaging. Nozzle scans were performed using a Nikon Metrology 225 kV Ultra-Focus CT system containing a 16-bit Perkin Elmer XRD1620 detector panel. The scans were run at 220 kV and the time was approximately 20 minutes per nozzle. Voxel resolution for each nozzle was 28.5 um. Rendering of the scans was conducted using VGStudiMAX2.2.

Results and Discussion

Figure 3 shows the current profiles of each injector used for the experiments presented in this paper. As mentioned, an oscilloscope was used to measure the current profile at 1 us time steps and the injector settings are listed in Table 1. For both energizing times of 0.45 ms and 0.7 ms, the current profiles match between the different injectors and was repeatable. Both time durations show similar profiles; however, the final set current of 11 A is reduced for the 0.7 ms duration. Figure 4 shows the rate of injection profiles for all 3 injectors at energizing times of 0.45 ms and 0.7 ms, respectively. For the duration of 0.7 ms, all 3 injectors rate of injection profiles start and end near the same times. However, for the shorter duration of 0.45 ms, as shown in Figure 4 (a), the 6-hole injection rate appears to end before the 1-hole and 2-hole. Further work is underway to address this behavior. Even though this behavior is observed with the injection analyzer and the injection rates appear different, the measured mass exiting the nozzle is similar to the measured mass from the scale method as highlighted in Table 2. Figure 4 also shows the average current during the injection event. The average current plotted in Figure 4 is sampled through the injection analyzer system. The results of the average current are similar between each injector for both energizing time durations.

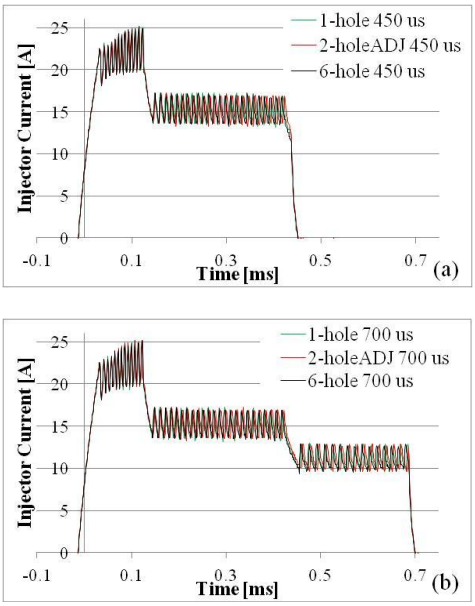

Figure 3. High-resolution current profiles for: (a) 450 us and (b) 700 us durations.

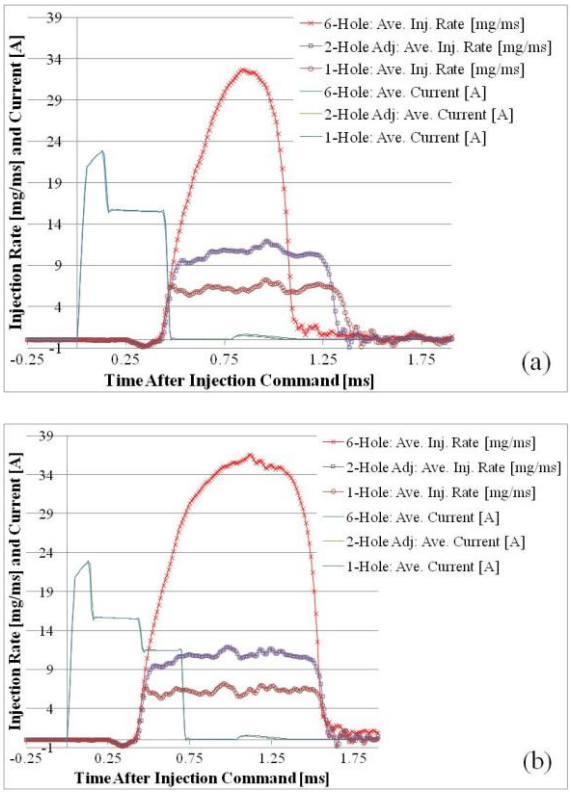

Figure 4. Rate of injection profiles for: (a) 450 us duration and (b) 700 us duration.

Table 2 shows the results of the injected fuel mass from the injection analyzer and the scale method. Initially, fuel mass was measured with an IAV injection analyzer utilizing the Bosch tube method. It was expected that the fuel mass would scale with the

increase in the number of orifices, considering the fuel injectors were driven with identical current profiles. Results show that the scaling expectation does not hold for the injectors. For example, between the 1-hole and 2-hole, the injected fuel mass for the 2-hole at 450 us duration is 1.5 times the amount of mass for the 1-hole, and 1.6 times for the 700 us duration. Similar observations were noted comparing the 2-hole to the 6-hole for the 450 us duration; however, at the larger duration of 700 us, the 6-hole was 2.7 times the amount of fuel as the 2-hole.

In order to eliminate the probability that the injection analyzer was the cause of the discrepancy, additional testing was conducted with a high-precision scale to measure the fuel mass. The scale method, as mentioned previously, is an average of 200 shots and is not a measurement of each shot to shot. Caution was taken to not allow any fuel to escape from the collection container during injection. Table 2 shows the results of measuring the fuel mass with the scale. Comparing the two mass measuring methods, similar results are present, thus providing confidence that the measurements with the injection analyzer are proper. Internal flow geometries are different between the 1-hole and the 2-hole/6-hole, with the fuel exiting at the tip for the 1-hole and exiting the sides for the 2-hole/6-hole. These different flow patterns may contribute to the non-linear scaling effect observed. The 2-hole nozzle fuel mass may be affected by uneven pressure near the needle due to the fuel exiting on one side of the nozzle. Clearly, from the results shown, the fuel mass does not linearly scale according to the number of injector holes.

Main Duration [us]	Rail Pressure [bar]	1-Hole: Inj. Analyzer 100 Shot Average [mg/shot]	1-Hole: Scale 200 Shot Average [mg/shot]
450	1000	5.74	5.23
700	1000	7.05	6.65

Main Duration [us]	Rail Pressure [bar]	2-Hole Adj: Inj. Analyzer 100 Shot Average [mg/shot]	2-Hole Adj: Scale 200 Shot Average [mg/shot]
450	1000	8.62	8.08
700	1000	11.52	11.41

Main Duration [us]	Rail Pressure [bar]	6-Hole: Inj. Analyzer 100 Shot Average [mg/shot]	6-Hole: Scale 200 Shot Average [mg/shot]
450	1000	15.03	14.21
700	1000	31.33	32.07

Table 2. Fuel mass from the injection analyzer and scale method for the 1-hole, 2-hole, and 6-hole injector.

Results of the liquid and vapor penetration lengths for the 1-hole, 2-hole, and 6-hole injectors are presented in Figures 5-7. In the figures, graph (a) represents the 0.45 ms duration and graph (b) represents the longer duration of 0.7 ms. Error bars on the graphs are the standard error in the measurement corresponding to the following relation, $\pm 2\sigma/\sqrt{N}$, where σ is the standard deviation and N is the number of experiments. For the standard error calculation, 5 experiments were conducted for each data point. Figure 5 shows the average penetration lengths for the 1-hole injector. The fuel quantity injected per shot was 5.74 mg and 7.05 mg for the 0.45 ms and 0.7 ms duration, respectively. After the transient stage, quasi-steady state occurs at approximately 0.20 ms after the start of injection, with a liquid length of 20 mm, for both durations. The vapor penetration length continues to increase after liquid length stabilizes.

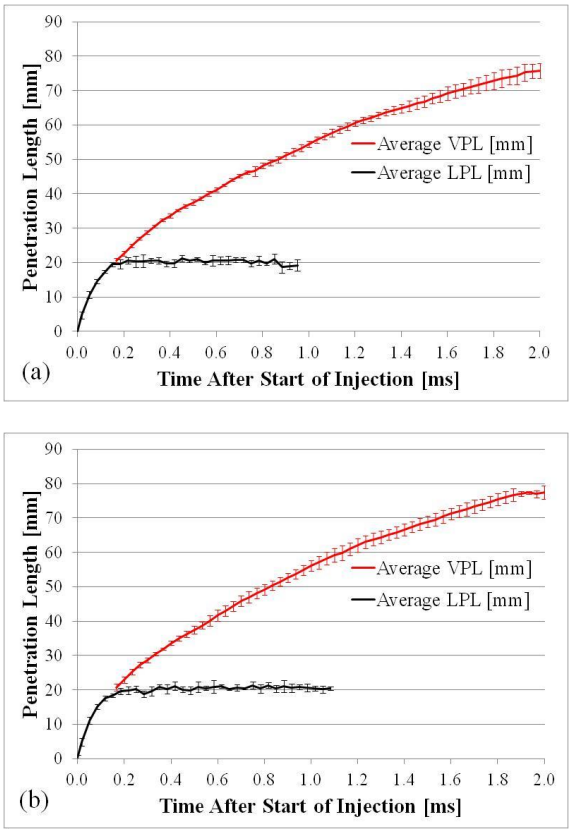

Figure 5. Liquid and vapor penetration lengths for the 1-hole inj., for durations of (a) 0.45 ms, (b) 0.7 ms.

The average liquid and vapor penetration lengths for the 2-hole injector are plotted in Figure 6. Only the vertical plume for the 2-hole injector is plotted in Figure 6, as the adjacent hole was behind the vertical plume during imaging. The total fuel quantity injected from both orifices was 8.62 mg and 11.52 mg for the 0.45 ms and 0.7 ms durations, respectively. Per orifice, an average of 4.31 mg, and 5.76 mg, was injected for each duration of 0.45 ms and 0.7 ms, respectively. For both injection durations, liquid length approaches a

quasi-steady state length of 15 mm at approximately 0.20 ms after the start of injection. The injected fuel mass between the 0.45 ms duration for the 1-hole and the fuel mass of the 0.7 ms case, for each orifice, is similar. However, the liquid penetration lengths are clearly different with the 2-hole injector being approximately 5 mm shorter. Unlike the 1-hole case, an increase in variability is present in the liquid penetration length. During analysis of the raw images, the liquid length appears to increase in one frame, and then decrease in the next. The vapor penetration length continues to steadily increase after liquid penetration reaches quasi-steady state. To note, at approximately 0.85 ms after start of injection, the vapor penetration length reaches the limit of the viewing area within the high temperature pressure vessel. In Figure 6, the vapor penetration length appears to reach a steady state; however, this is due to the viewing limit of the chamber and it is expected that the vapor penetration length would continue to increase.

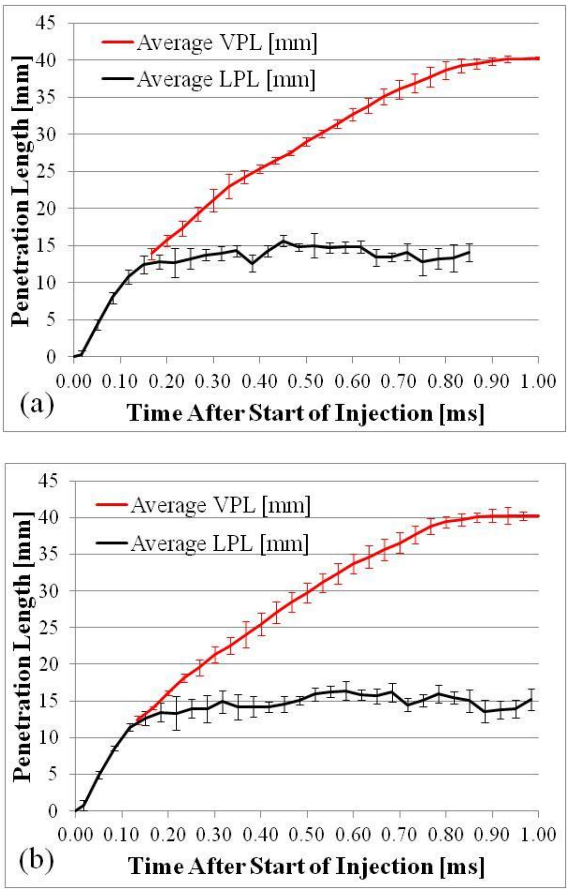

Figure 6. Liquid and vapor penetration lengths for the 2-hole inj., for durations of (a) 0.45 ms, (b) 0.7 ms.

Figure 7 shows the liquid and vapor penetration lengths for the 6-hole injector. Similarly with the 2-hole injector, one vertical plume was analyzed for the results presented. The total fuel quantity injected from all 6 orifices was 15.03 mg and 31.33 mg for the 0.45 ms and 0.7 ms duration, respectively. This corresponds to approximately 2.5 mg and 5.2 mg per shot for each orifice and for each duration. The rate that the penetration increases is lower for the 6-hole than compared to the 1-hole and 2-hole injectors. For both durations, quasi-steady liquid penetration length occurs at a much longer time of approximately 0.45 ms after start of injection compared to the 1-hole and 2-hole injectors.

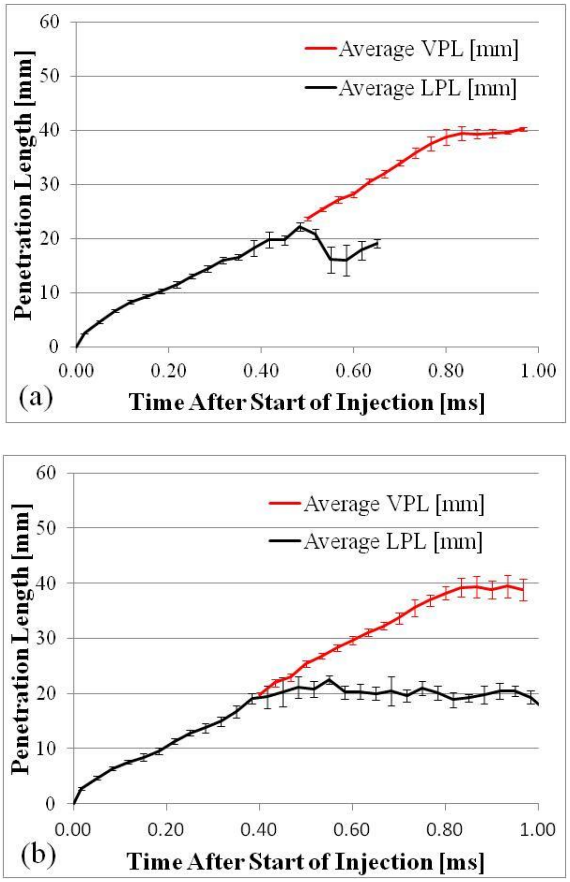

Figure 7. Liquid and vapor penetration lengths for the 6-hole inj., for durations of (a) 0.45 ms, (b) 0.7 ms.

The injected fuel per orifice for the 0.7 ms duration is similar to that of the 2-hole, 0.7 ms duration case, 5.22 mg and 5.76 mg. However, the 6-hole liquid penetration length is longer than the liquid penetration length for the 2-hole. Also noticeable is a sudden decrease in liquid penetration length for the 6-hole injector near 0.5 ms. In this time regime, fluctuations in the liquid penetration lengths were present. Eccentric needle lift can be a contributing factor in the variations observed in penetration lengths. The vapor penetration length continued to increase once the liquid penetration length reached quasi-steady state. The rate of vapor penetration growth is similar to the rate of liquid length growth for the 6-hole injector. However,

the vapor penetration rate tends to decrease with the 1-hole and 2-hole injectors. As with the 2-hole injector, the 6-hole vapor penetration length reaches the outer limit of the viewing area in the HTPV near 0.85 ms after start of injection.

As mentioned earlier, additional experiments were conducted from the axial position for the 2-hole and 6-hole injectors. During these experiments only the liquid portion of the spray was imaged with Mie scattering diagnostics with the high-speed camera operating at 80,000 fps. With this orientation and higher frame rate more details of the spray dynamics can be observed. Figures 8 and 9 show the results for the 2-hole and 6-hole injectors for both injection durations of 0.45 ms and 0.7 ms. In addition, plotted on the graphs is the liquid penetration length from the previously mentioned Mie and schlieren experiments. This is denoted as Top M&S in the legend. For the axial Mie scattering experiments both spray plumes for the 2-hole are plotted. For the 6-hole injector experiments, only the two plumes that have the similar orientation of the 2-hole injector are plotted. Figure 8 (a) shows the 2 plumes for the 0.45 ms duration. Both plumes have similar transient behavior; however, the quasi-steady liquid penetration length is longer by approximately 2 mm throughout the steady regime. In addition, since the frame rate is much higher for these sets of experiments, fluctuations in liquid penetration length can be observed. For the 0.7 ms duration case, as shown in Figure 8 (b), similar transient behavior is present, and there is less variability in the quasi-steady state regime. The liquid penetration length from the Mie and schlieren experiments is in general agreement with the presented axial results.

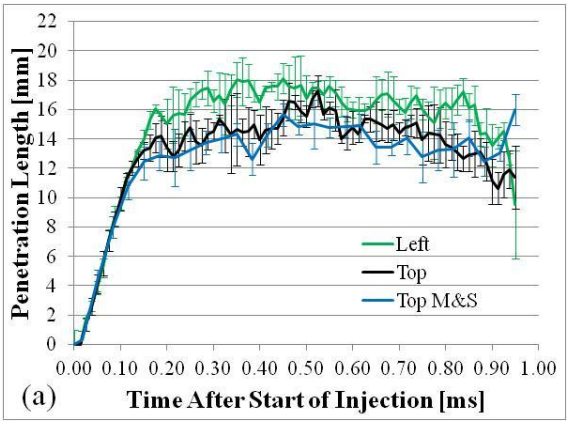

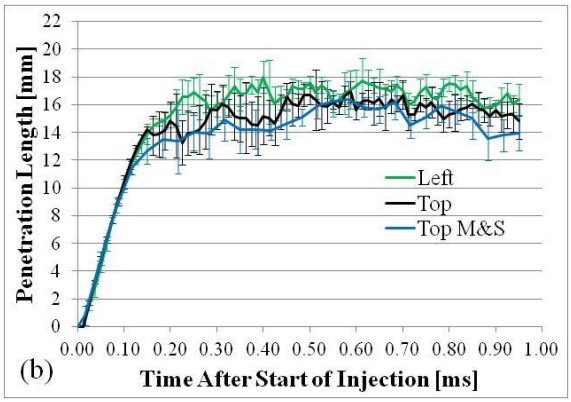

Figure 8. Liquid penetration lengths for the 2-hole injector, for durations of (a) 0.45 ms, (b) 0.7 ms.

Figure 9 shows the liquid penetration length from the 6-hole injector. In addition, the vertical plume, identified as Top M&S, from the Mie and schlieren experiments is also plotted. The quasi-steady liquid penetration lengths for both durations are approximately 20 mm. However, significant variations in penetration length are observed. An interesting observation from the experiments is that at approximately 0.35 ms after the start of injection, a decrease in liquid length occurs. This behavior could be attributed to non-uniform pressure regions and/or uneven flow patterns inside the nozzle caused by needle wobble. Analyzing the images from the Mie experiments, this behavior is evident. The spray plume length grows and then at this time, the length decreases, and then suddenly increases up to the quasi-steady state regime. As mentioned, variations were observed with the 2-hole injector; however, not as significant as with the 6-hole injector.

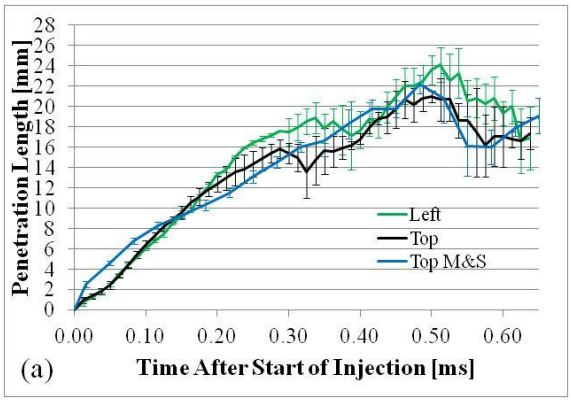

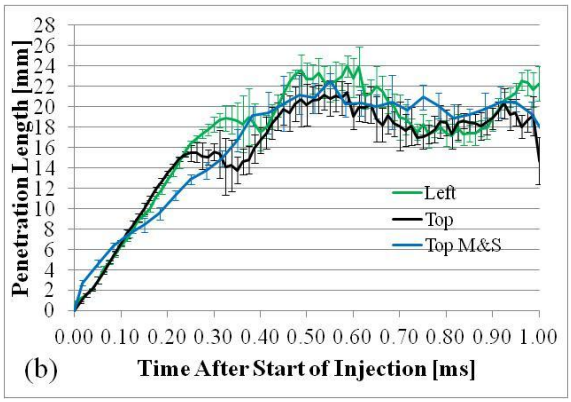

Figure 9. Liquid penetration lengths for the 6-hole injector, for durations of (a) 0.45 ms, (b) 0.7 ms.

Figures 10 and 11 show the processed images for the Mie and schlieren experiments with all injectors and the axial Mie experiments for the 2-hole and 6-hole injectors. The images presented are for the 0.7 ms injection duration case. The vertical plume is the plume oriented to the left in the images for Figure 10 and for Figure 11 the vertical plume is oriented vertically. For both figures, the liquid regime appears dark on the images, whereas the vapor regime in Figure 10 appears lighter. Visual analysis of the image sets to investigate plume to plume interaction reveal that the plumes tend to not interact with one another.

CFD Results

For the 1-hole nozzle study, the numerical results show very good agreement with the liquid phase penetration profiles as shown in Figure 12. The discrepancies observed in vapor phase profiles are due to the vapor length calculation model that presently only accounts for the prevalent single component fuel (and not the mixture). Because the surrogate is composed of 80% n-dodecane and 20% tri-methyl-benzene, we can expect variations with the measured data.

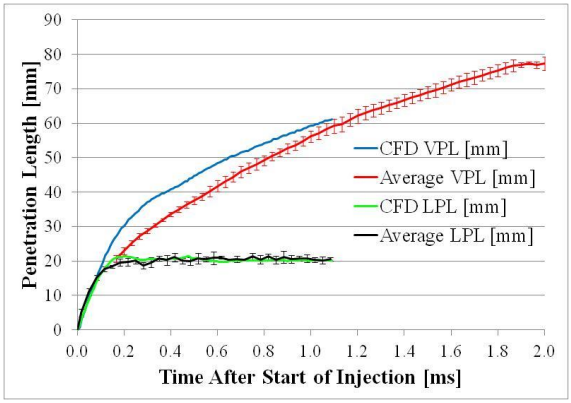

Figure 12. Comparison of exp. and CFD penetration lengths for the 1-hole injector for 0.7 ms duration.

The multi-hole nozzle (two orifice) data is presented in Figure 13 for the vertical spray plume and is compared to experimental results. The modeling results show variations in liquid penetration length when compared to experiments. When comparing to 1-hole peak liquid penetration magnitude (20 mm), the 2-hole model shows no apparent effect maintaining the approximately same value of 20 mm. Physically this would indicate that the nozzle orifice distance (1 mm) and spacing of 60° prevents them from interacting in this configuration. Current work is underway to investigate this effect further and determine whether this issue is numerical or is a realistic representation of the physics. However, the physical behavior, spray structure and propagation is captured accurately by the model. Similar observations are made with vapor phase profiles, where the model's ability to calculate vapor line based on fuel mass fraction of the mixture will be addressed. Figure 14 shows the comparison of CFD images with the experimental images for both the 1-hole and 2-hole, 0.7 ms injection duration. In addition, modeling work with the 6-hole injector is underway.

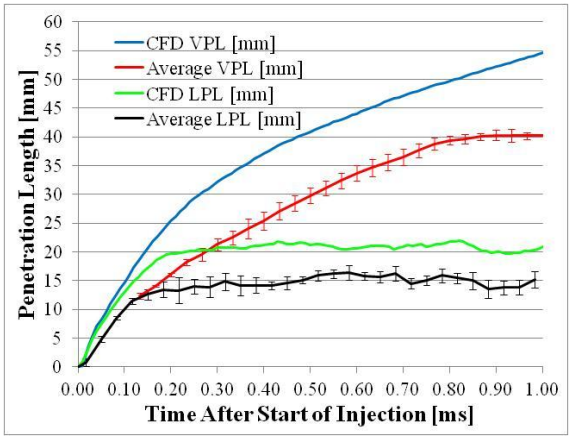

Figure 13. Comparison of exp. and CFD penetration lengths for the 2-hole injector for 0.7 ms duration.

Results of the CT imaging are shown in Figure 15. The top row highlights the rendering of the CT scans while the bottom row shows a CT scan bisecting through the orifices. Figure 15 (a) shows the slice of the 1-hole nozzle. In the image, it is clear that the needle is not fully engaged inside the nozzle. All three nozzles were disassembled from the injector body for testing, and the 1-hole needle was not fully inserted into the nozzle during the CT scan. Furthermore, the orientation of the axial hole drilled into the end of the 1-hole nozzle is not in the center. In both Figure 15 (a) and (b), the welds on the outside of the nozzle are visible and there is no indication that any weld protrudes more than halfway into an orifice. The rendered image for the 6-hole, top of Figure 15 (c), shows 3 visible orifices. The other 3 orifices are not

viewable in the current orientation. In addition, the top rendered images show the orientation of the injector nozzle inside the HTPV during testing. Other slices and views of the internal geometry of the injector nozzles are under analysis to reveal variations that may lead to differences observed in the results presented in this study. Overall, the CT images will be useful in determining variations of internal geometry.

Conclusions

In this work, JP-8 spray experiments were conducted at elevated pressure and temperature with Mie and schlieren diagnostics to investigate nozzle configurations with a 1-hole, 2-hole, and 6-hole Bosch CRIN3 fuel injector at two different fuel injection durations consisting of 0.45 ms and 0.7 ms. Liquid and vapor penetration lengths for the injectors were acquired. In addition, a CFD study was conducted to compare the penetration lengths for the 1-hole and 2-hole fuel injectors. Findings from this study are as follows:

- Fuel mass does not scale linearly with the increase in the number of orifices between injectors.
- At the conditions tested, the 1-hole and 6-hole injectors both have a quasi-steady liquid penetration length of 20 mm. The 2-hole injector has a liquid penetration length of 15 mm.
- The injected fuel mass for the 0.45 ms duration of the 1-hole injector was similar to that of the 0.7 ms duration of the 2-hole injector. However, the liquid penetration lengths are clearly different with the 2-hole injector being approximately 5 mm shorter.
- The rate of penetration length between the 1-hole and 2-hole injectors was similar based on visual analysis of the data. However, the penetration length rate for the 6-hole injector was slower.
- The quasi-steady state liquid length for the 2-hole injector varied by 2 mm between plumes.
- The 6-hole injector had significant more variations in liquid length than the 1-hole and 2-hole injectors.
- CFD studies for 1-hole liquid length show good agreement with liquid and vapor lengths and were useful in extracting spray kinematics. However, differences are observed for the 2-hole liquid length when compared to experiments, with the model predicting a value of 20 mm for both plumes. Both CFD vapor profiles show a general trend but improvements to the model will simulate the experimental results to a higher degree.
- CT scans will aid in characterizing internal geometry of injector nozzles.

Acknowledgements

This research was supported in part by an appointment to the U.S. Army Research Laboratory Postdoctoral Fellowship program administered by Oak Ridge Associated Universities through a contract with the U.S. Army Research Laboratory.

We gratefully acknowledge the computing resources provided on "Pershing", a 1260 node (20,160 cores, 40 TB of memory) computer cluster operated by U.S. Army Research Laboratory Department of Defense Super Computing Resource Center (ARL-DSRC).

In addition, we would like to acknowledge Dr. Tim Edwards of the Air Force Research Laboratory for supplying the JP-8.

References

1. Reitz, R.D., *Combustion and Flame* 160:1-8 (2013).
2. Kweon, C.-B.M., "A Review of Heavy-Fueled Rotary Engine Combustion Technologies," US Army Research Laboratory Technical Report, ARL-TR-5546, May 2011.
3. Pickett, L.M., Genzale, C.L., Bruneaux, G., Malbec, L.-M., Hermant, L., Christiansen, C., Schramm, J., *SAE* 2010-01-2106 (2010).
4. Bazyn, T., and Martin, G.C., *23rd Annual Conference on Liquid Atomization and Spray Systems*, Ventura, California, May 2011.
5. Meijer, M., Somers, B., Johnson, J., Naber, J., Lee, S.-Y., Malbec, L.M., Bruneaux, G., Pickett, L.M., Bardi, M., Payri, R., Bazyn, T., *Atomization and Sprays* 22:777–806 (2012).
6. Siebers, D.L., *SAE* 980809 (1998).
7. Pickett, L.M., and Hoogterp, L., *SAE* 2008-01-1083 (2008).
8. Kook, S., and Pickett, L.M., *Fuel* 93:539-548 (2012).
9. Nesbit, J.E., Naber, J.D., Lee, S.-Y., Kurtz, E., Ge, H.-W., Robarge, N., *23rd Annual Conference on Liquid Atomization and Spray Systems*, Ventura, California, May 2011.
10. Kastengren, A.L., Tilocco, F.Z., Powell, C.F., Manin, J., Pickett, L.M., Payri, R., Bazyn, T., *Atomization and Sprays* 22:1011-1052 (2012).
11. Malbec, L.-M., Egusquiza, J., Bruneaux, G., Meijer, M., *SAE* 2013-24-0037 (2013).
12. Parrish, S.E., and Zink, R.J., *23rd Annual Conference on Liquid Atomization and Spray Systems*, Ventura, California, May 2011.
13. Pickett, L.M., Kook, S., Williams, T.C., *SAE* 2009-01-0658 (2009).
14. Bravo, L., Kurman, M., Kweon, C., *Submitted to the 26th Annual Conference on Liquid Atomization and Spray Systems*, Portland, Oregon, May 2014.
15. Senecal, P.K., Pomraning, E., Xue, Q., Som, S., Banerjee, S., Hu, B., Liu, K., Deur, J.M., *Proceedings of the ASME 2013 Internal Combustion Engine Division Fall Technical Conference*, Dearborn, Michigan, October 2013.

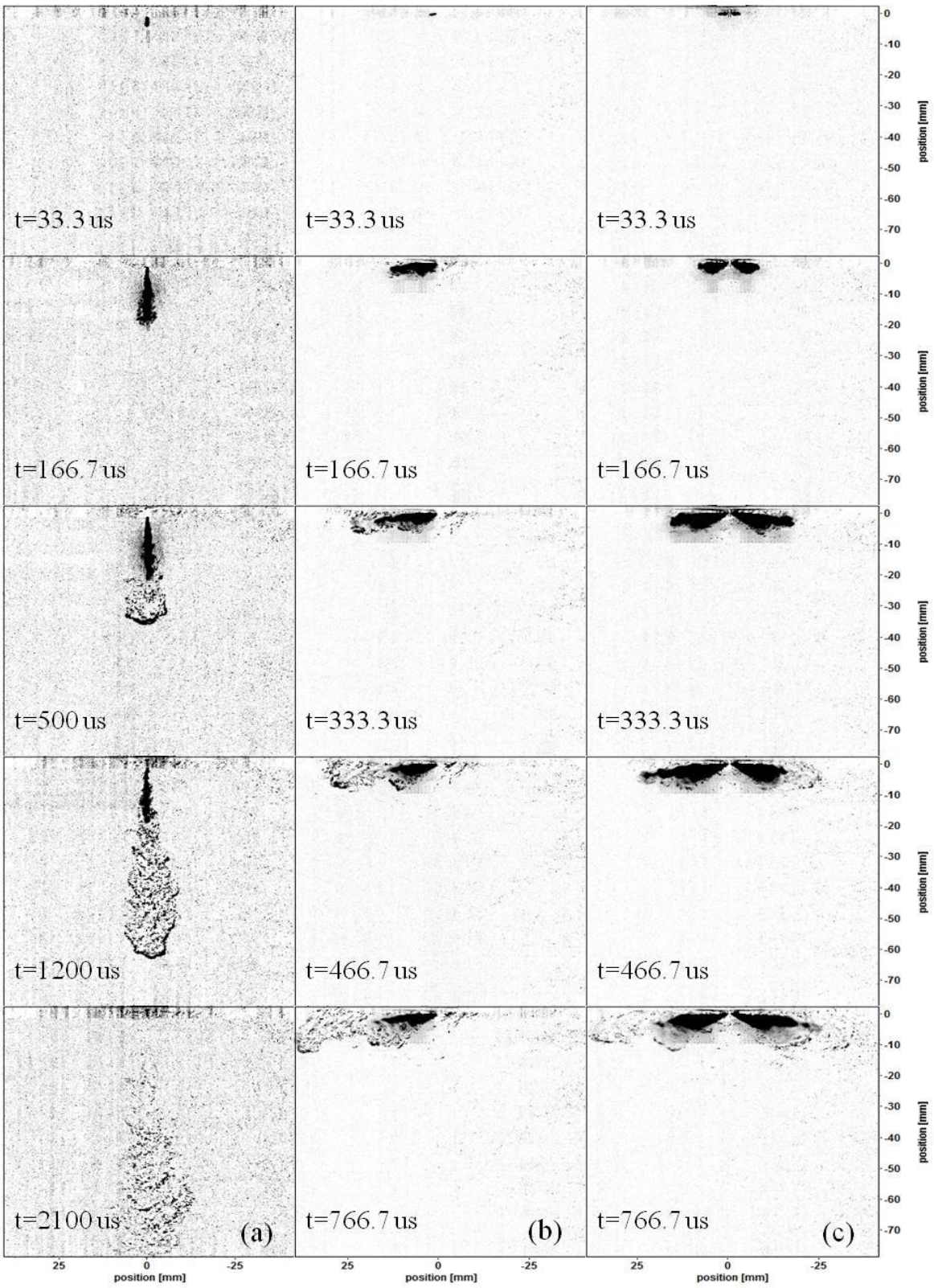

Figure 10. Comparison of experimental Mie and schlieren overlay images for: (a) 1-hole, (b) 2-hole, and (c) 6-hole injectors with injection duration of 0.7ms.

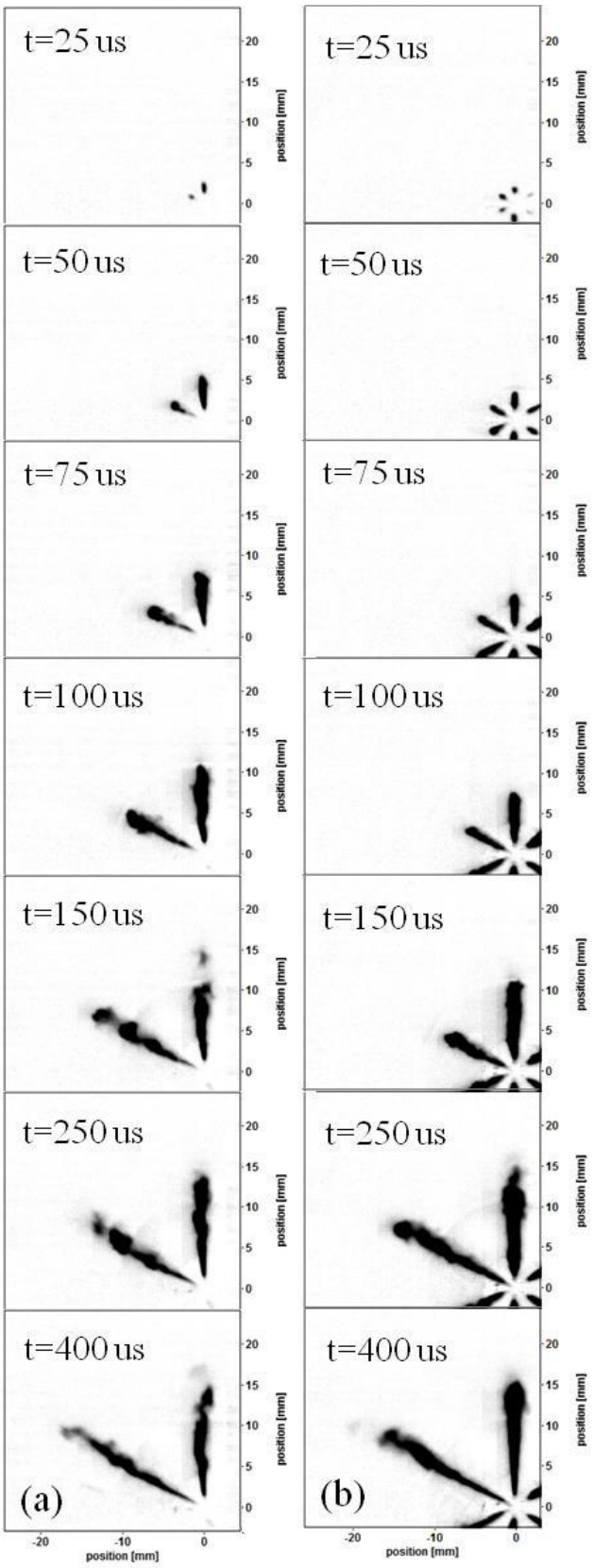

Figure 11. Comparison of exp. Mie images for: (a) 2-hole and (b) 6-hole injectors with injection duration of 0.7ms.

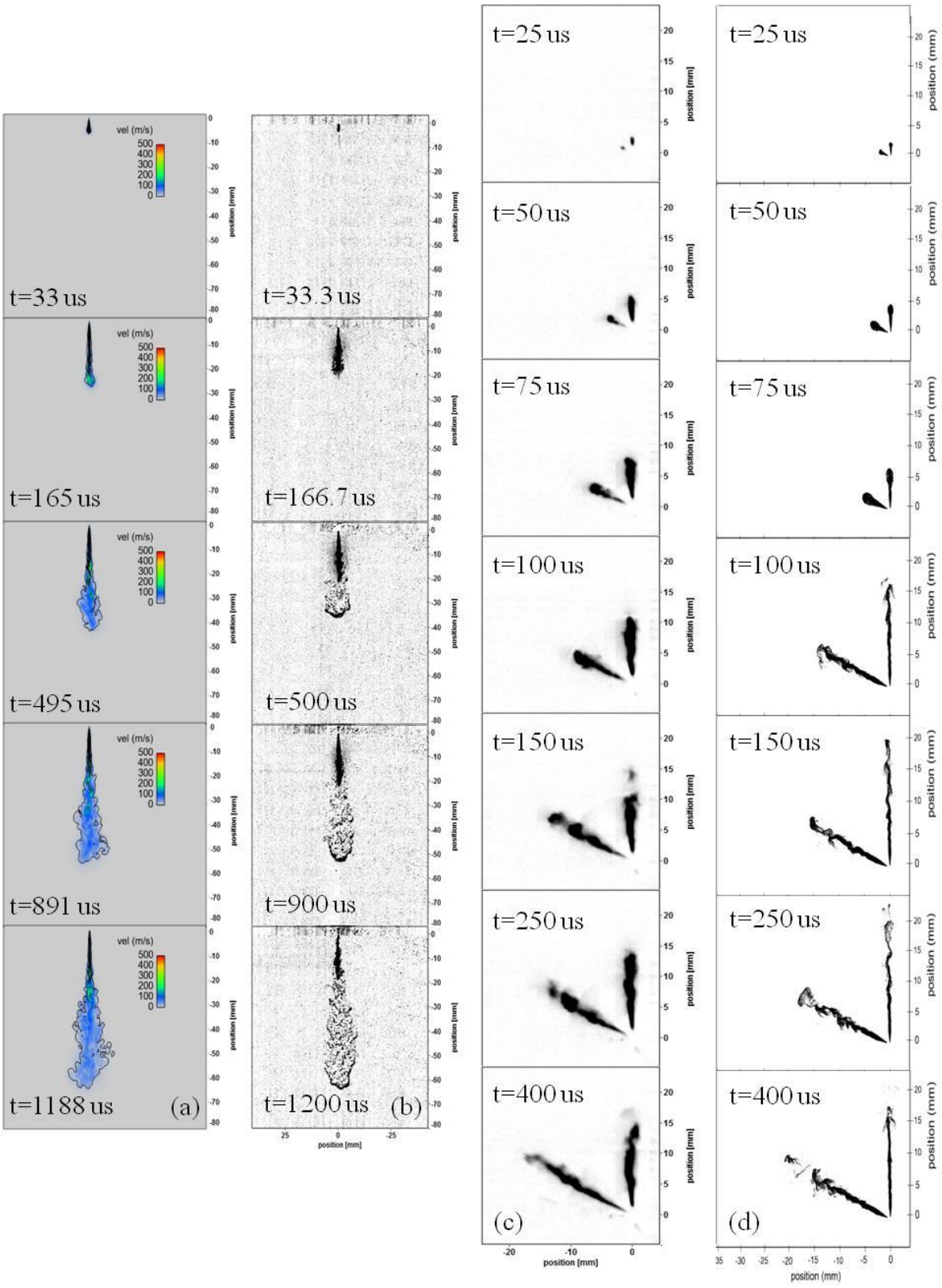

Figure 14. CFD comparison to exp. images in columns: (a) 1-hole CFD, (b) 1-hole exp., (c) 2-hole exp., (d) 2-hole CFD.

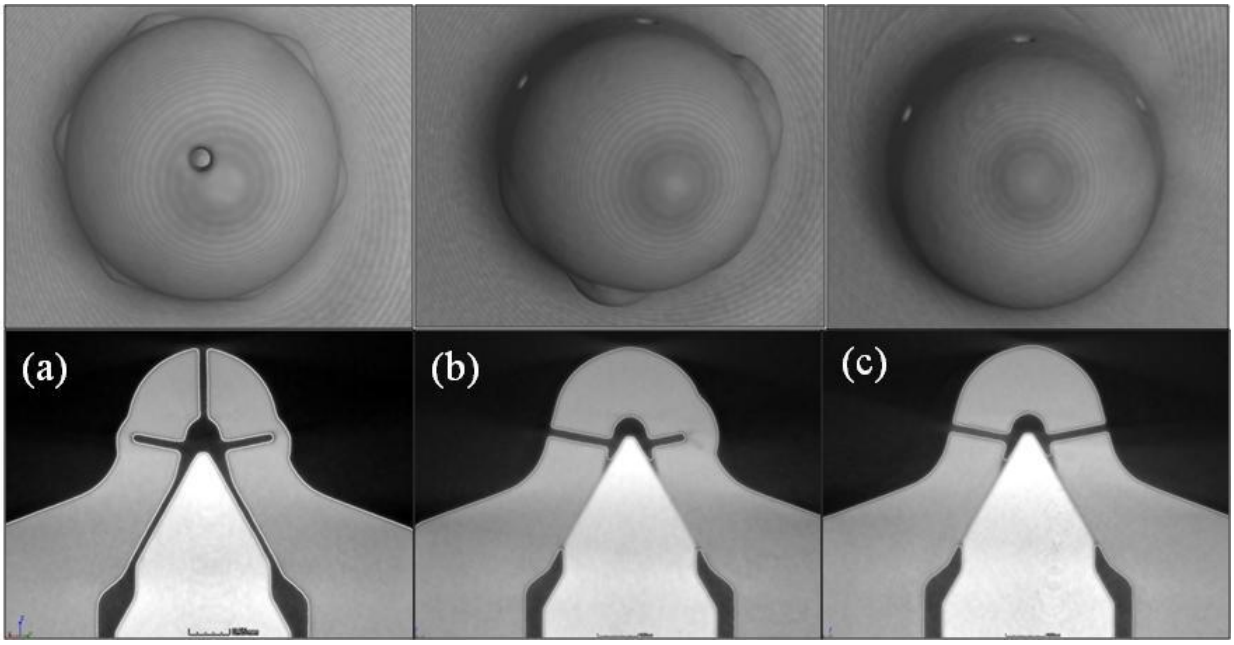

Figure 15. Select rendered CT scans (top) and CT slices (bottom) for the fuel injectors: (a) 1-hole, (b) 2-hole, (c) 6-hole.

1 (PDF)	DEFENSE TECHNICAL INFORMATION CTR DTIC OCA
2 (PDF)	DIRECTOR US ARMY RESEARCH LAB RDRL CIO LL IMAL HRA MAIL & RECORDS MGMT
1 (PDF)	GOVT PRINTG OFC A MALHOTRA
4 (PDF)	DIR USARL RDRL VTP L BRAVO M KURMAN C-B KWEON M TESS

INTENTIONALLY LEFT BLANK.